Published in final edited form as:

Cell Rep. 2018 May 15; 23(7): 1907–1914. doi:10.1016/j.celrep.2018.04.058.

Loss of a Negative Regulator of mTORC1 Induces Aerobic Glycolysis and Altered Fiber Composition in Skeletal Muscle

Paul A. Dutchak[1,2,3], **Sandi J. Estill-Terpack**[1], **Abigail A. Plec**[1], **Xiaozheng Zhao**[1], **Chendong Yang**[4], **Jun Chen**[1], **Bookyung Ko**[4], **Ralph J. Deberardinis**[4], **Yonghao Yu**[1], and **Benjamin P. Tu**[1,*,5]

[1]Department of Biochemistry, University of Texas Southwestern Medical Center, Dallas, TX, USA

[2]Department of Psychiatry and Neuroscience, Université Laval, Québec, QC, Canada

[3]CERVO Brain Research Centre, 2601 Chemin de la Canardiére, Québec, QC, Canada

[4]Children's Medical Center Research Institute, University of Texas Southwestern Medical Center, Dallas, TX, USA

SUMMARY

The conserved GATOR1 complex consisting of NPRL2-NPRL3-DEPDC5 inhibits mammalian target of rapamycin complex 1 (mTORC1) in response to amino acid insufficiency. Here, we show that loss of NPRL2 and GATOR1 function in skeletal muscle causes constitutive activation of mTORC1 signaling in the fed and fasted states. Muscle fibers of NPRL2 knockout animals are significantly larger and show altered fiber-type composition, with more fast-twitch glycolytic and fewer slow-twitch oxidative fibers. NPRL2 muscle knockout mice also have altered running behavior and enhanced glucose tolerance. Furthermore, loss of NPRL2 induces aerobic glycolysis and suppresses glucose entry into the TCA cycle. Such chronic activation of mTORC1 leads to compensatory increases in anaplerotic pathways to replenish TCA intermediates that are consumed for biosynthetic purposes. These phenotypes reveal a fundamental role for the GATOR1 complex in the homeostatic regulation of mitochondrial functions (biosynthesis versus ATP) to mediate carbohydrate utilization in muscle.

In Brief

*Correspondence: enjamin.tu@utsouthwestern.edu.
[5]Lead Contact

SUPPLEMENTAL INFORMATION

Supplemental information includes Supplemental Experimental Procedures, four figures, and three tables and can be found with this article online at https://doi.org/10.1016/j.celrep.2018.04.058.

AUTHOR CONTRIBUTIONS

This study was conceived by P.A.D. and B.P.T. P.A.D. led the study and performed most of the experiments. S.J.E.-T. and A.A.P. assisted with mouse genotyping and husbandry. A.A.P. and S.J.E.-T. assisted with tissue harvesting, dissections, and western blot analysis. X.Z. and Y.Y. performed TMT proteomic analyses. C.Y., B.K., and R.J.D. performed ^{13}C-glucose infusions and analysis of metabolism in muscle tissue by GC-MS/MS. J.C. assisted with targeted LC-MS/MS metabolite profiling. The paper was written by P.A.D. and B.P.T. and has been approved by all authors.

DECLARATIONS OF INTERESTS

R.J.D. is an adviser for Agios Pharmaceuticals.

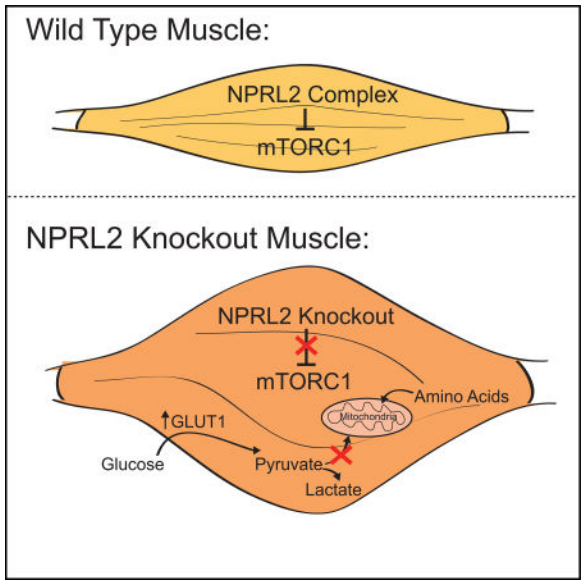

Dutchak et al. investigate how mTORC1 activation rewires cellular metabolism in skeletal muscle by analyzing the consequences of loss of NPRL2, a component of the GATOR1 complex that is a conserved negative regulator of mTORC1.

INTRODUCTION

Skeletal muscle constitutes approximately 40% of the total mass of adult humans, providing a means for movement and posturing at the expense of cellular energy (Zurlo et al., 1990). Different fiber types within skeletal muscle preferentially rely on distinct metabolic pathways to meet their energy demands and consequently show hallmarks of oxidative or glycolytic metabolism (Zierath and Hawley, 2004). The homeostatic regulators of energy metabolism in distinct fiber types ensure energy requirements are met during ranges of physical activities, from rest to exertion (Allen et al., 2008; Westerblad et al., 2010).

The mammalian target of rapamycin complex 1 (mTORC1) signaling pathway is a dynamic regulator of protein translation and cellular metabolism that responds to growth factor signaling and amino acid availability (Shimobayashi and Hall, 2014, 2016). mTORC1 activity is regulated by interactions with lysosomal guanosine triphosphate (GTP)-binding proteins called RHEB and RAGs (Efeyan et al., 2013; Sancak et al., 2010). Insulin and growth factor signaling pathways stimulate pro-growth effects and control energy metabolism by activating the phosphatidylinositol 3-kinase/AKT signal transduction pathway, which inhibits the guanosine triphosphatase (GTPase)-activating function of TSC1/2 toward RHEB and permits mTORC1 activation (Inoki et al., 2002; Tee et al., 2002). Regulation of mTORC1 activity is also responsive to nutrient-sensing pathways that contribute to metabolic homeostasis and growth. Amino acids are sensed by an evolutionarily conserved protein complex that is present from yeast to humans (Dokudovskaya et al., 2011; Wu and Tu, 2011). This complex consists of NPRL2, NPRL3, and DEPDC5, collectively termed GATOR1, and functions as a GTPase-activating protein

for small RAG GTPases to inhibit mTORC1 during amino acid limitation (Bar-Peled et al., 2013; Dutchak et al., 2015; Neklesa and Davis, 2009; Panchaud et al., 2013).

Inhibition of mTORC1 results in general translational repression (Choo et al., 2008; Gingras et al., 2001) and activation of autophagy (Jung et al., 2010) to maintain nutrients and energy for survival. In skeletal muscle, mTORC1 is inhibited during starvation or exercise to permit activation of autophagy and recycling of metabolites for energy (Castets et al., 2013; He et al., 2012). Loss of mTORC1 function, by deletion of RAPTOR, leads to progressive muscle atrophy with impaired oxidative capacity (Bentzinger et al., 2008). In contrast, constitutive activation of mTORC1 by deletion of the TSC1/2 growth factor signaling branch stimulates glycolytic gene expression and downregulates PGC1α, a master transcriptional coactivator of mitochondrial biogenesis (Bentzinger et al., 2013; Düvel et al., 2010; Liu et al., 2014; Puigserver et al., 1998).

The presence of both amino acid- and growth factor-dependent inputs into the regulation of mTORC1 makes it difficult to predict the physiological contribution of the amino acid-sensing pathway alone. Here we show that skeletal muscle-specific deletion of NPRL2, a critical component of the GATOR1 complex, increases fast-twitch, type II glycolytic muscle fibers and induces a switch to a highly glycolytic metabolism. These findings reveal how activation of mTORC1 rewires metabolism in a manner that necessitates increased glucose utilization in the skeletal muscle, thereby contributing to glucose homeostasis *in vivo* (Doi et al., 2007; Kleinert et al., 2011). We further show how loss of this conserved, negative regulator of TORC1 results in enhanced anaplerosis alongside enhanced mTORC1 signaling to replenish tricarboxylic acid (TCA) cycle intermediates that are consumed during proliferative metabolism.

RESULTS

NPRL2 mKO Mice Show Altered Muscle Fiber Composition and mTORC1 Activity

To determine the function of the GATOR1 complex in skeletal muscle, we created a muscle-specific knockout by breeding $Nprl2^{loxp/loxp}$ with $Myod^{icre/WT}$ mice to delete *Nprl2* from the skeletal muscle lineage (Chen et al., 2005; Dutchak et al., 2015). qRT-PCR verified that *Nprl2* mRNA was deleted from all skeletal muscle groups examined, but not from other tissues, including liver and adipose (Figure 1A). Western blot analysis was used to determine the expression of all GATOR1 components: NPRL2, NPRL3, and DEPDC5 in wild-type (WT); $Nprl2^{loxp/WT}$: $Myod^{icre/WT}$ (NPRL2 mHET); and $Nprl2^{loxp/loxp}$: $Myod^{icre/WT}$ (NPRL2 mKO). Expression of NPRL2 was not detected in NPRL2 mKO, whereas NPRL3 and DEPDC5 were expressed at similar amounts across genotypes (Figure 1B).

We performed histological analysis of muscle sections to determine whether the loss of NPRL2 resulted in a phenotypic change in the tissue. H&E-stained sections showed a significant increase in fiber size in NPRL2 mKO, consistent with known anabolic effects of mTORC1 activation (Figures 1C and S1A). Immunohistochemical staining of myosin heavy chain (MHC)-I, a marker of type I oxidative fibers, showed a dramatic decrease in the number of stained cells in the NPRL2 mKO soleus compared to WT (Figures 1C and S1B). Metachromatic staining also showed fewer type I oxidative fibers in the NPRL2 mKO

(Figure 1C), suggesting that loss of NPRL2 can elicit a fiber-type switch that results in fewer type I oxidative fibers and more type II glycolytic muscle fibers.

To determine whether NPRL2 contributed to the physiological regulation of mTORC1 in the muscle, we analyzed mTORC1 signaling in the fed and fasted states. Western blot analysis of phosphorylated S6 kinase (S6K1), a downstream target of mTORC1, showed significantly more phosphorylation in the soleus of NPRL2 mKO compared to WT in the fed state (Figure 1D). S6K1 phosphorylation was not decreased in the fasted NPRL2 mKO, consistent with the idea that NPRL2 is important to repress mTORC1 during nutrient limitation *in vivo*. Consistent with high mTORC1 activity, conversion of LC3-I to LC3-II did not occur in fasted NPRL2 mKO, suggestive of impaired autophagy (Figure 1D). Because mTORC1 activity can also be regulated by the AKT:TSC1/2 growth factor-dependent pathway, we analyzed the phosphorylation status of active AKT in these tissues. Surprisingly, western blot analysis showed a substantial reduction of AKT phosphorylation at S473, but not T308, in the NPRL2 mKO compared to WT during the fasted state and the fed state (Figures 1D and S1C). These data suggest the existence of a negative feedback mechanism to limit pAKT-S473 in response to loss of NPRL2 and activation of amino acid signaling into mTORC1. Activation of mTORC1 is known to repress upstream signaling through feedback mechanisms, such as through the phosphorylation of IRS1, Grb10, or Sin1, which could be enhanced in NPRL2 mKO (Harrington et al., 2004; Hsu et al., 2011; Liu et al., 2013; Shah and Hunter, 2006; Yu et al., 2011). Nonetheless, these data indicate that loss of GATOR1 function is sufficient to result in hallmarks of hyperactive TORC1 signaling despite the presence of an intact TSC1/2 complex.

NPRL2 mKO Mice Show Altered Running Behavior and Carbohydrate Metabolism

Skeletal muscle autophagy has been shown to contribute to energy metabolism in mice during acute periods of activity (He et al., 2012). We hypothesized that constitutive activation of mTORC1, and impaired autophagy, may therefore alter the running behavior of the NPRL2 mKO. We performed wheel-running experiments, allowing mice free access to wheels over a 12 hr light-to-dark cycle. Despite slightly decreased mass of the NPRL2 mKO animals and no difference in body composition (Figures 2A and S2A–S2C), they showed more wheel-running activity during the first 18 min following the switch from light to dark (Figure 2B), whereas no significant difference in total activity over the light-to-dark cycle was observed (Figure 2C). Moreover, we did not observe any change in wheel-running behavior of the NPRL2 mHET compared to WT (Figures S2D and S2E). These data are consistent with increased abundance of fast-twitch muscle fibers in the NPRL2 mKO.

Fast-twitch, type II muscle fibers rely heavily on glycolytic metabolism for energy production. We hypothesized that the altered fiber composition of the NPRL2 mKO may increase the demand for carbohydrate metabolism and subsequently show an altered respiratory exchange ratio (RER). Metabolic cage studies showed NPRL2 mKO mice had significantly higher RER during the dark cycle compared to WT mice (Figure 2D). Quantitatively, VCO_2/VO_2 measurements of the NPRL2 mKO reached values of 1, indicating a preference for carbohydrate utilization during this period. These observations prompted us to examine glucose tolerance in the mice. Animals were challenged with an

intraperitoneal glucose tolerance test, and the clearance of glucose from the blood was determined. NPRL2 mKO mice showed a significantly greater rate of glucose clearance, despite no difference in glucose-induced insulin secretion (Figures 2E and 2F). We also measured plasma lactate, a product of glycolysis, during the glucose challenge. We found significantly lower blood lactate levels of the NPRL2 mKO only after glucose injection compared to WT, indicating that deleting NPRL2 from the muscle is sufficient to alter utilization of glycolytic end products systemically (Figure 2G).

Loss of NPRL2 Reprograms Metabolic Pathways in Muscle to Promote Aerobic Glycolysis

To determine whether NPRL2 deletion from skeletal muscle tissue altered the expression of proteins that control metabolism and fiber-type composition, we used isobaric labeling (tandem mass tag [TMT]) quantitative mass spectrometry (Hu et al., 2016) to measure protein amounts in extracts from the WT and NPRL2 mKO soleus muscle (Figures 3A and S3A). Consistent with histological analysis, protein mass spectrometry of NPRL2 mKO fibers showed significantly reduced abundance of proteins whose expression is restricted to slow-twitch fibers, including Tnnc1 (troponin C1), Tnni1 (troponin I1), Tnnt1 (troponin T1), Myl3 (myosin light chain 3), and Myh7 (myosin heavy chain 7) (Figure S3A). Decreased expression of myosin heavy chain 2B (Myh4) in the NPRL2 mKO suggested the NPRL2 mKO muscle fibers are enriched for type IIa, fast-twitch oxidative fibers (Murgia et al., 2015). The altered abundance of various muscle-specific proteins assessed by mass spectrometry is consistent with the observed reduction in type I oxidative fibers and increase in type II fast-twitch glycolytic fibers in NPRL2 mKO mice.

Altered glucose metabolism in the NPRL2 mKO mice prompted us to investigate the mechanism by which NPRL2 contributes to glucose homeostasis in the muscle. We used qRT-PCR to analyze gene expression of glycolytic and mitochondrial-related genes in the NPRL2 mKO muscle and observed a significant decrease in PGC1α mRNA, suggesting a defect in mitochondrial biogenesis, consistent with previous observations in the TSC1 muscle knockout (Figure 3B) (Bentzinger et al., 2013). In contrast, the expression of genes involved in glucose uptake was significantly increased, including glucose transporter 1 (*Glut1*) and hexokinase 2 (*Hk2*) (Figure 3B). Expression of *Glut4*, the insulin-dependent glucose transporter, was not changed (Figure 3B). Total muscle glycogen content was minimally changed (Figures 3C, S3B, and S3C), whereas glycogen synthase was preferentially phosphorylated at the inhibitory Ser641 site in the NPRL2 mKO only during fasting (Figure S3D). Lactate dehydrogenase B (*Ldhb*) expression was also increased 2-fold, suggestive of increased glycolytic metabolism.

Entry of glucose-derived carbon into the TCA cycle is largely controlled by the activity of the pyruvate dehydrogenase complex, which is negatively regulated by phosphorylation. Western blot analysis of the inhibitory phosphorylation site on pyruvate dehydrogenase component E1A (Ser293) showed significantly more phosphorylation in the NPRL2 mKO compared to WT, despite no change in PDHE1A protein abundance (Figure 3D). We used qRT-PCR to measure the expression of pyruvate dehydrogenase kinases *Pdk1–Pdk4* in soleus muscle and determined that *Pdk3* expression was significantly increased in the

NPRL2 mKO muscle (Figure 3E). Collectively, these data suggest that mitochondrial utilization of pyruvate for energy is decreased by the loss of NPRL2 and GATOR1 function.

To assess the metabolic utilization of glucose in the skeletal muscle tissue, we performed ^{13}C-glucose labeling experiments. Mice were injected intraperitoneally with ^{13}C-glucose, and its conversion to TCA cycle metabolites was measured by gas chromatography-mass spectrometry (GC-MS). We observed a significant decrease in fractional labeling of TCA cycle intermediates, including citrate and fumarate, in the NPRL2 mKO muscle tissues (Figures 3F and 3G). We also performed ^{13}C-glucose steady-state infusion experiments to measure production of the glycolytic intermediates 3-phosphoglycerate, pyruvate, and lactate. NPRL2 mKO animals showed significantly higher fractional enrichment of these glycolytic metabolites in the soleus tissue compared to WT (Figure 3H). As a surrogate for pyruvate dehydrogenase's relative contribution to supplying glucose-derived carbon to the TCA cycle in WT and mKO mice, we compared the enrichment of glycolytic intermediates upstream of pyruvate dehydrogenase (PDH) to enrichment in citrate downstream of PDH (Grassian et al., 2011). Consistent with the enhanced *Pdk3* expression and pyruvate dehydrogenase phosphorylation in the mKO, these muscles had significantly elevated labeling ratios in all measured glycolytic intermediates (Figure S3E). No significant differences were observed in the labeling of these metabolites in liver or serum (Figures S3F and S3G). Collectively, multiple lines of evidence are consistent with the notion that activation of mTORC1 through loss of NPRL2 in muscle induces aerobic glycolysis, which is accompanied by reduced glucose entry into the TCA cycle.

Loss of NPRL2 Results in a Compensatory Increase in Anaplerotic Pathways that Replenish the TCA Cycle

We then looked beyond glucose metabolism to assess how other metabolic pathways might be altered in NPRL2 mKO. We used targeted mass spectrometry to measure the relative abundance of metabolites in WT and NPRL2 knockout (KO) soleus tissue, as well as plasma. Quantification of amino acids showed significantly reduced abundance of glutamine and aspartate only in muscle tissue, not in blood (Figures 4A and 4B). Although a trend of higher citrate or isocitrate abundance was observed by mass spectrometry, no significant difference was observed in the abundance of TCA cycle intermediates (Figure 4C). Aspartate and glutamine are derived from TCA cycle intermediates and are consumed for both protein synthesis and nucleotide synthesis. These data are consistent with previous findings in yeast showing that TORC1 activation promotes the synthesis and subsequent utilization of these nitrogen-containing amino acids for proliferative metabolism (Chen et al., 2017; Laxman et al., 2014). Furthermore, proteomic analysis revealed increased abundance of the Glud1 (glutamate dehydrogenase) and Glul (glutamine synthetase) enzymes that are required for glutamine synthesis from α-ketoglutarate, as well as increased amounts of GOT1 (aspartate aminotransferase), which is required for aspartate synthesis from oxaloacetate and serves as a source of glutamate from α-ketoglutarate (Figure 3A). Because aspartate and glutamine are required for *de novo* purine and pyrimidine synthesis, these findings are also consistent with the previously reported role for mTORC1 in stimulating both purine and pyrimidine synthesis (Ben-Sahra et al., 2013, 2016; Robitaille et al., 2013)

Unexpectedly, given the well-known role for mTORC1 in the activation of protein translation (Ma and Blenis, 2009), no obvious increases in the amounts of ribosomal proteins or translation factors were observed from our unbiased proteomic analyses of NPRL2 mKO soleus tissue, despite evidence of increased pS6K1 (Figure 1D). Instead, we observed a striking enrichment in proteins involved in amino acid and fatty acid catabolism that were increased in abundance in NPRL2mKOsoleus (Figure S4). These included enzymes important for mitochondrial and peroxisomal function (Figures 3A and S4). Nearly every enzyme involved in branched amino acid catabolism (Bcat2, Bckdha, Bckdhb, Dbt, Ivd, Acad8, Aldh6a1, and Mccc1) exhibited increased abundance in NPRL2 mKO. Numerous enzymes involved in other aspects of amino acid metabolism and fatty acid oxidation were also increased in NPRL2 mKO (Figure S4).

Examination of each of these enzymes reveals that most are involved in anaplerotic reactions that replenish mitochondrial TCA cycle intermediates (Figure 4E). Because activation of TORC1 promotes the consumption of TCA cycle intermediates for the synthesis of nitrogen-containing amino acids aspartate and glutamine (Chen et al., 2017), we interpret these findings to indicate that chronic activation of mTORC1 leads to compensatory increase in these anaplerotic pathways to help replenish these TCA cycle intermediates (Figure 4E). Consistent with increased degradation of branched-chain amino acids, we observed lower blood plasma amounts of leucine, isoleucine, and valine in NPRL2 mKO animals (Figure 4B). To further assess whether NPRL2 mKO animals have increased general amino acid catabolism, urine samples were collected and urea content was analyzed. NPRL2 mKO animals excrete significantly more urea in their urine, consistent with increased amino acid catabolism (Figure 4C). Collectively, our findings on the phenotypes of NPRL2 mKO indicate that activation of mTORC1 in skeletal muscle promotes aerobic glycolysis and the utilization of the mitochondria for biosynthetic purposes, specifically the synthesis of non-essential nitrogen-containing amino acids. This leads to a compensatory increase in numerous amino acid and fatty acid degradative pathways that help replenish the TCA cycle intermediates for mitochondrial energy production.

DISCUSSION

The numerous regulatory pathways that modulate mTORC1 activity indicate its central role in controlling cell growth and maintaining cellular homeostasis. Genetic studies of the TSC1/2 growth factor regulatory pathway have shown constitutive activation of mTORC1 can affect global metabolic changes and elicit late-onset myopathies (Bentzinger et al., 2013; Castets et al., 2013; Guridi et al., 2015). Here we show the evolutionarily conserved, NPRL2-dependent GATOR1 complex is also necessary to repress mTORC1 activity *in vivo*. Consistent with loss of TSC1/2 in the soleus muscle, loss of NPRL2 causes constitutive activation of mTORC1 and larger muscle fibers. We show profound changes in muscle fiber-type composition in the NPRL2 mKO, with increased numbers of fast-twitch, type II glycolytic muscle fibers.

We also provide evidence that the GATOR1 complex contributes to integrative metabolism in the skeletal muscle. Similar to TSC1 mKO, NPRL2 mKO mice have increased sensitivity to glucose challenge (Guridi et al., 2015). Our data suggest that loss of NPRL2 alters the fate

of glucose metabolism, consistent with mTORC1 activation (Düvel et al., 2010). Despite no change in glycogen content between WT and NPRL2 KO, the contribution of glucose oxidation to the TCA cycle was suppressed by distinct mechanisms, including increased expression of lactate dehydrogenase and phosphorylation of the pyruvate dehydrogenase complex. Although these are also hallmarks of hypoxia-inducible (HIF)-1α activation, whose translation is subject to control by mTORC1 (Hudson et al., 2002), the induction of glycolytic metabolism caused by loss of NPRL2 *in vivo* appears to be independent of HIF transcription factors, because both HIF-1α and HIF-2α were undetectable at the protein level in soleus of both WT and NPRL2 mKO. Moreover, skeletal muscle deletion of HIF-1α did not result in notable changes in soleus fiber-type composition (Mason et al., 2004).

It is now clear why TORC1 activation promotes aerobic glycolysis and increased glucose utilization. In budding yeast, we have shown that TORC1 activation promotes the synthesis of the amino acids aspartate and glutamine from the mitochondria (Chen et al., 2017; Laxman et al., 2014). Aspartate and glutamine are nitrogen-containing forms of TCA cycle intermediates, which are subsequently consumed for synthesis of nitrogen-containing metabolites important for growth, such as nucleotides, NAD^+, and glutathione. Because TCA cycle intermediates are being consumed for biosynthesis, cells must appropriately increase glycolysis to meet cellular demands for ATP. In NPRL2 mKO, we observed lower amounts of aspartate and glutamine, suggestive of increased consumption of these amino acids, as well as increased abundance of enzymes involved in aspartate, glutamine, and glutathione synthesis (Figure 4E). Such rewiring of metabolism is highly reminiscent of metabolic phenotypes observed following disruption of GATOR1 function in yeast. Therefore, the utilization of mitochondria for biosynthesis necessitates an upregulation of glycolysis, which might represent the basis of the Warburg effect observed in so many proliferating cell types.

In support of this idea, through unbiased quantitative mass spectrometry, we observed elevated expression of enzymes in the soleus of NPRL2 mKO involved in anaplerotic reactions of the mitochondrial TCA cycle. This was the most striking signature we observed in terms of changes in tissue protein abundance (Figure 4). Their function is to replenish TCA intermediates through the catabolism of amino acids and fatty acids. These data suggest increased catabolism of amino acids and are supported by our observation that urea excretion in the NPRL2 mKO is increased; they also suggest lower abundance of amino acids in the muscle tissue. Collectively, these observations suggest that chronic activation of mTORC1 results in a metabolic compensation toward these anaplerotic reactions, consistent with the idea that proliferating cells require a high anaplerotic flux (DeBerardinis et al., 2008). We also noted lower levels of branched amino acids in plasma of NPRL2 mKO animals, pointing to a special role for branched-chain amino acid degradation in the context of reduced glucose oxidation. For the TCA cycle to support growth, there must be a source of both anaplerosis and acetyl-coenzyme A (CoA). Leucine degradation could provide a source of acetyl-CoA to offset reduced PDH activity, while degradation of isoleucine and valine provides an anaplerotic flux. Therefore, increased branched-chain amino acid catabolism may be a compensatory consequence of mTORC1 activation due to the anaplerotic potential of these amino acids.

Furthermore, we previously showed that NPRL2 KO mouse embryonic fibroblasts (MEFs) exhibit a defect in the processing of vitamin B12 (cobalamin) in response to starvation (Dutchak et al., 2015), which results in a defect in methionine homeostasis. Besides methionine synthase, vitamin B12 is required for the complete catabolism of the branched amino acids isoleucine and valine for them to serve as productive anaplerotic substrates (Figure 4). Vitamin B12 is a required cofactor for methylmalonyl-CoA mutase in the conversion to propionyl-CoA to succinyl-CoA, which can then feed into the TCA cycle. This and our previous study together show how a core metabolic function of the GATOR1 complex in response to starvation is to promote anaplerotic reactions that replenish TCA cycle intermediates. Vitamin B12 uptake and processing are key components of this program, allowing particular amino acids and fatty acids to participate in anaplerosis. In times of nutritional stress, the TCA cycle intermediates must be conserved so that they can be used for ATP synthesis.

In summary, we have shown that NPRL2 and the GATOR1 complex regulate the composition of glycolytic and oxidative muscle fibers *in vivo*. These results show how this amino acid-sensing pathway influences the utilization of various nutrient fuels by the TCA cycle. We conclude that the GATOR1 complex coordinates anabolic and catabolic pathways to regulate carbohydrate utilization and mitochondrial homeostasis in tune with the amino acid status of cells.

EXPERIMENTAL PROCEDURES

Animal Experiments

Mice were maintained in a 12/12 hr light/dark cycle at a temperature of 22°C and fed standard chow (Harlan, No. 2016) *ad libitum*. NPRL2 mKO mice were generated using the $Nprl2^{loxp/+}$ mice described previously (Dutchak et al., 2015). $Nprl2^{loxp/+}$ mice were crossed with $Myod^{icre/WT}$ (Chen et al., 2005) to generate muscle-specific heterozygous animals. Heterozygous KO animals were backcrossed to C57BL/6 mice for at least three generations, with subsequent crosses with $Nprl2^{loxp/+}$ and $Nprl2^{loxp/loxp}$ animals, resulting in the control mice ($Nprl2^{loxp/loxp}$ and $Nprl2^{loxp/+}$), NPRL2 mHET mice ($Nprl2^{loxp/+}$: $Myod^{icre/WT}$), and NPRL2 mKO mice ($Nprl2^{loxp/loxp}$: $Myod^{icre/WT}$) that were used for these studies. Genotypes of animals were determined by PCR, with primers listed in Table S1. All animal experiments were approved by the Institutional Animal Research Advisory Committee of the University of Texas Southwestern Medical Center at Dallas. Male mice were used in all experiments.

Statistical Analysis

Statistical analysis was performed by two-tailed Student’s t test using Microsoft Excel 2010. A p value of < 0.05 was considered significant. Supplemental Experimental Procedures contains additional experimental procedures.

Supplementary Material

Refer to Web version on PubMed Central for supplementary material.

Acknowledgments

This work was supported by grants from CPRIT (RP140655 to B.P.T.), a research fellowship from CPRIT (to P.A.D.), the Welch Foundation (I-1797 to B.P.T.), and the NIH (R01 CA185169 to B.P.T., R01 GM114160 to Y.Y., and R01 CA157996 to R.J.D.).

References

Allen DG, Lamb GD, Westerblad H. Skeletal muscle fatigue: cellular mechanisms. Physiol. Rev. 2008; 88:287–332. [PubMed: 18195089]

Bar-Peled L, Chantranupong L, Cherniack AD, Chen WW, Ottina KA, Grabiner BC, Spear ED, Carter SL, Meyerson M, Sabatini DM. A tumor suppressor complex with GAP activity for the Rag GTPases that signal amino acid sufficiency to mTORC1. Science. 2013; 340:1100–1106. [PubMed: 23723238]

Ben-Sahra I, Howell JJ, Asara JM, Manning BD. Stimulation of *de novo* pyrimidine synthesis by growth signaling through mTOR and S6K1. Science. 2013; 339:1323–1328. [PubMed: 23429703]

Ben-Sahra I, Hoxhaj G, Ricoult SJH, Asara JM, Manning BD. mTORC1 induces purine synthesis through control of the mitochondrial tetrahydrofolate cycle. Science. 2016; 351:728–733. [PubMed: 26912861]

Bentzinger CF, Romanino K, Cloëtta D, Lin S, Mascarenhas JB, Oliveri F, Xia J, Casanova E, Costa CF, Brink M, et al. Skeletal muscle-specific ablation of raptor, but not of rictor, causes metabolic changes and results in muscle dystrophy. Cell Metab. 2008; 8:411–424. [PubMed: 19046572]

Bentzinger CF, Lin S, Romanino K, Castets P, Guridi M, Summermatter S, Handschin C, Tintignac LA, Hall MN, Rüegg MA. Differential response of skeletal muscles to mTORC1 signaling during atrophy and hypertrophy. Skelet. Muscle. 2013; 3:6. [PubMed: 23497627]

Castets P, Lin S, Rion N, Di Fulvio S, Romanino K, Guridi M, Frank S, Tintignac LA, Sinnreich M, Rüegg MA. Sustained activation of mTORC1 in skeletal muscle inhibits constitutive and starvation-induced autophagy and causes a severe, late-onset myopathy. Cell Metab. 2013; 17:731–744. [PubMed: 23602450]

Chen JC, Mortimer J, Marley J, Goldhamer DJ. MyoD-cre transgenic mice: a model for conditional mutagenesis and lineage tracing of skeletal muscle. Genesis. 2005; 41:116–121. [PubMed: 15729689]

Chen J, Sutter BM, Shi L, Tu BP. GATOR1 regulates nitrogenic cataplerotic reactions of the mitochondrial TCA cycle. Nat. Chem. Biol. 2017; 13:1179–1186. [PubMed: 28920930]

Choo AY, Yoon SO, Kim SG, Roux PP, Blenis J. Rapamycin differentially inhibits S6Ks and 4E-BP1 to mediate cell-type-specific repression of mRNA translation. Proc. Natl. Acad. Sci. USA. 2008; 105:17414–17419. [PubMed: 18955708]

DeBerardinis RJ, Lum JJ, Hatzivassiliou G, Thompson CB. The biology of cancer: metabolic reprogramming fuels cell growth and proliferation. Cell Metab. 2008; 7:11–20. [PubMed: 18177721]

Doi M, Yamaoka I, Nakayama M, Sugahara K, Yoshizawa F. Hypoglycemic effect of isoleucine involves increased muscle glucose uptake and whole body glucose oxidation and decreased hepatic gluconeogenesis. Am. J. Physiol. Endocrinol. Metab. 2007; 292:E1683–E1693. [PubMed: 17299083]

Dokudovskaya S, Waharte F, Schlessinger A, Pieper U, Devos DP, Cristea IM, Williams R, Salamero J, Chait BT, Sali A, et al. A conserved coatomer-related complex containing Sec13 and Seh1 dynamically associates with the vacuole in Saccharomyces cerevisiae. Mol. Cell. Proteomics. 2011; 10 M110.006478.

Dutchak PA, Laxman S, Estill SJ, Wang C, Wang Y, Wang Y, Bulut GB, Gao J, Huang LJ, Tu BP. Regulation of hematopoiesis and methionine homeostasis by mTORC1 inhibitor NPRL2. Cell Rep. 2015; 12:371–379. [PubMed: 26166573]

Düvel K, Yecies JL, Menon S, Raman P, Lipovsky AI, Souza AL, Triantafellow E, Ma Q, Gorski R, Cleaver S, et al. Activation of a metabolic gene regulatory network downstream of mTOR complex 1. Mol. Cell. 2010; 39:171–183. [PubMed: 20670887]

Efeyan A, Zoncu R, Chang S, Gumper I, Snitkin H, Wolfson RL, Kirak O, Sabatini DD, Sabatini DM. Regulation of mTORC1 by the Rag GTPases is necessary for neonatal autophagy and survival. Nature. 2013; 493:679–683. [PubMed: 23263183]

Gingras AC, Raught B, Sonenberg N. Regulation of translation initiation by FRAP/mTOR. Genes Dev. 2001; 15:807–826. [PubMed: 11297505]

Grassian AR, Metallo CM, Coloff JL, Stephanopoulos G, Brugge JS. Erk regulation of pyruvate dehydrogenase flux through PDK4 modulates cell proliferation. Genes Dev. 2011; 25:1716–1733. [PubMed: 21852536]

Guridi M, Tintignac LA, Lin S, Kupr B, Castets P, Rüegg MA. Activation of mTORC1 in skeletal muscle regulates whole-body metabolism through FGF21. Sci. Signal. 2015; 8:ra113. [PubMed: 26554817]

Harrington LS, Findlay GM, Gray A, Tolkacheva T, Wigfield S, Rebholz H, Barnett J, Leslie NR, Cheng S, Shepherd PR, et al. The TSC1-2 tumor suppressor controls insulin-PI3K signaling via regulation of IRS proteins. J. Cell Biol. 2004; 166:213–223. [PubMed: 15249583]

He C, Bassik MC, Moresi V, Sun K, Wei Y, Zou Z, An Z, Loh J, Fisher J, Sun Q, et al. Exercise-induced BCL2-regulated autophagy is required for muscle glucose homeostasis. Nature. 2012; 481:511–515. [PubMed: 22258505]

Hsu PP, Kang SA, Rameseder J, Zhang Y, Ottina KA, Lim D, Peterson TR, Choi Y, Gray NS, Yaffe MB, et al. The mTOR-regulated phosphoproteome reveals a mechanism of mTORC1-mediated inhibition of growth factor signaling. Science. 2011; 332:1317–1322. [PubMed: 21659604]

Hu R, Huffman KE, Chu M, Zhang Y, Minna JD, Yu Y. Quantitative Secretomic Analysis Identifies Extracellular Protein Factors That Modulate the Metastatic Phenotype of Non-Small Cell Lung Cancer. J. Proteome Res. 2016; 15:477–486. [PubMed: 26736068]

Hudson CC, Liu M, Chiang GG, Otterness DM, Loomis DC, Kaper F, Giaccia AJ, Abraham RT. Regulation of hypoxia-inducible factor 1alpha expression and function by the mammalian target of rapamycin. Mol. Cell. Biol. 2002; 22:7004–7014. [PubMed: 12242281]

Inoki K, Li Y, Zhu T, Wu J, Guan KL. TSC2 is phosphorylated and inhibited by Akt and suppresses mTOR signalling. Nat. Cell Biol. 2002; 4:648–657. [PubMed: 12172553]

Jung CH, Ro SH, Cao J, Otto NM, Kim DH. mTOR regulation of autophagy. FEBS Lett. 2010; 584:1287–1295. [PubMed: 20083114]

Kleinert M, Liao YH, Nelson JL, Bernard JR, Wang W, Ivy JL. An amino acid mixture enhances insulin-stimulated glucose uptake in isolated rat epitrochlearis muscle. J. Appl. Physiol. 2011; 111:163–169. [PubMed: 21527668]

Laxman S, Sutter BM, Shi L, Tu BP. Npr2 inhibits TORC1 to prevent inappropriate utilization of glutamine for biosynthesis of nitrogen-containing metabolites. Sci. Signal. 2014; 7:ra120. [PubMed: 25515537]

Liu P, Gan W, Inuzuka H, Lazorchak AS, Gao D, Arojo O, Liu D, Wan L, Zhai B, Yu Y, et al. Sin1 phosphorylation impairs mTORC2 complex integrity and inhibits downstream Akt signalling to suppress tumorigenesis. Nat. Cell Biol. 2013; 15:1340–1350. [PubMed: 24161930]

Liu L, Nam M, Fan W, Akie TE, Hoaglin DC, Gao G, Keaney JF Jr, Cooper MP. Nutrient sensing by the mitochondrial transcription machinery dictates oxidative phosphorylation. J. Clin. Invest. 2014; 124:768–784. [PubMed: 24430182]

Ma XM, Blenis J. Molecular mechanisms of mTOR-mediated translational control. Nat. Rev. Mol. Cell Biol. 2009; 10:307–318. [PubMed: 19339977]

Mason SD, Howlett RA, Kim MJ, Olfert IM, Hogan MC, McNulty W, Hickey RP, Wagner PD, Kahn CR, Giordano FJ, Johnson RS. Loss of skeletal muscle HIF-1alpha results in altered exercise endurance. PLoS Biol. 2004; 2:e288. [PubMed: 15328538]

Murgia M, Nagaraj N, Deshmukh AS, Zeiler M, Cancellara P, Moretti I, Reggiani C, Schiaffino S, Mann M. Single muscle fiber proteomics reveals unexpected mitochondrial specialization. EMBO Rep. 2015; 16:387–395. [PubMed: 25643707]

Neklesa TK, Davis RW. A genome-wide screen for regulators of TORC1 in response to amino acid starvation reveals a conserved Npr2/3 complex. PLoS Genet. 2009; 5:e1000515. [PubMed: 19521502]

Panchaud N, Péli-Gulli MP, De Virgilio C. Amino acid deprivation inhibits TORC1 through a GTPase-activating protein complex for the Rag family GTPase Gtr1. Sci. Signal. 2013; 6:ra42. [PubMed: 23716719]

Puigserver P, Wu Z, Park CW, Graves R, Wright M, Spiegelman BM. A cold-inducible coactivator of nuclear receptors linked to adaptive thermogenesis. Cell. 1998; 92:829–839. [PubMed: 9529258]

Robitaille AM, Christen S, Shimobayashi M, Cornu M, Fava LL, Moes S, Prescianotto-Baschong C, Sauer U, Jenoe P, Hall MN. Quantitative phosphoproteomics reveal mTORC1 activates de novo pyrimidine synthesis. Science. 2013; 339:1320–1323. [PubMed: 23429704]

Sancak Y, Bar-Peled L, Zoncu R, Markhard AL, Nada S, Sabatini DM. Ragulator-Rag complex targets mTORC1 to the lysosomal surface and is necessary for its activation by amino acids. Cell. 2010; 141:290–303. [PubMed: 20381137]

Shah OJ, Hunter T. Turnover of the active fraction of IRS1 involves raptor-mTOR- and S6K1-dependent serine phosphorylation in cell culture models of tuberous sclerosis. Mol. Cell. Biol. 2006; 26:6425–6434. [PubMed: 16914728]

Shimobayashi M, Hall MN. Making new contacts: the mTOR network in metabolism and signalling crosstalk. Nat. Rev. Mol. Cell Biol. 2014; 15:155–162. [PubMed: 24556838]

Shimobayashi M, Hall MN. Multiple amino acid sensing inputs to mTORC1. Cell Res. 2016; 26:7–20. [PubMed: 26658722]

Tee AR, Fingar DC, Manning BD, Kwiatkowski DJ, Cantley LC, Blenis J. Tuberous sclerosis complex-1 and-2 gene products function together to inhibit mammalian target of rapamycin (mTOR)-mediated downstream signaling. Proc. Natl. Acad. Sci. USA. 2002; 99:13571–13576. [PubMed: 12271141]

Westerblad H, Bruton JD, Katz A. Skeletal muscle: energy metabolism, fiber types, fatigue and adaptability. Exp. Cell Res. 2010; 316:3093–3099. [PubMed: 20580710]

Wu X, Tu BP. Selective regulation of autophagy by the Iml1-Npr2-Npr3 complex in the absence of nitrogen starvation. Mol. Biol. Cell. 2011; 22:4124–4133. [PubMed: 21900499]

Yu Y, Yoon SO, Poulogiannis G, Yang Q, Ma XM, Villén J, Kubica N, Hoffman GR, Cantley LC, Gygi SP, Blenis J. Phosphoproteomic analysis identifies Grb10 as an mTORC1 substrate that negatively regulates insulin signaling. Science. 2011; 332:1322–1326. [PubMed: 21659605]

Zierath JR, Hawley JA. Skeletal muscle fiber type: influence on contractile and metabolic properties. PLoS Biol. 2004; 2:e348. [PubMed: 15486583]

Zurlo F, Larson K, Bogardus C, Ravussin E. Skeletal muscle metabolism is a major determinant of resting energy expenditure. J. Clin. Invest. 1990; 86:1423–1427. [PubMed: 2243122]

Highlights

- Deletion of NPRL2 results in increased type II fiber composition in soleus muscle
- NPRL2 is necessary to repress mTORC1 in soleus muscle during fasting
- Loss of NPRL2 increases pyruvate conversion to lactate and reduces pyruvate entry into TCA cycle
- NPRL2 coordinates glucose and amino acid metabolism

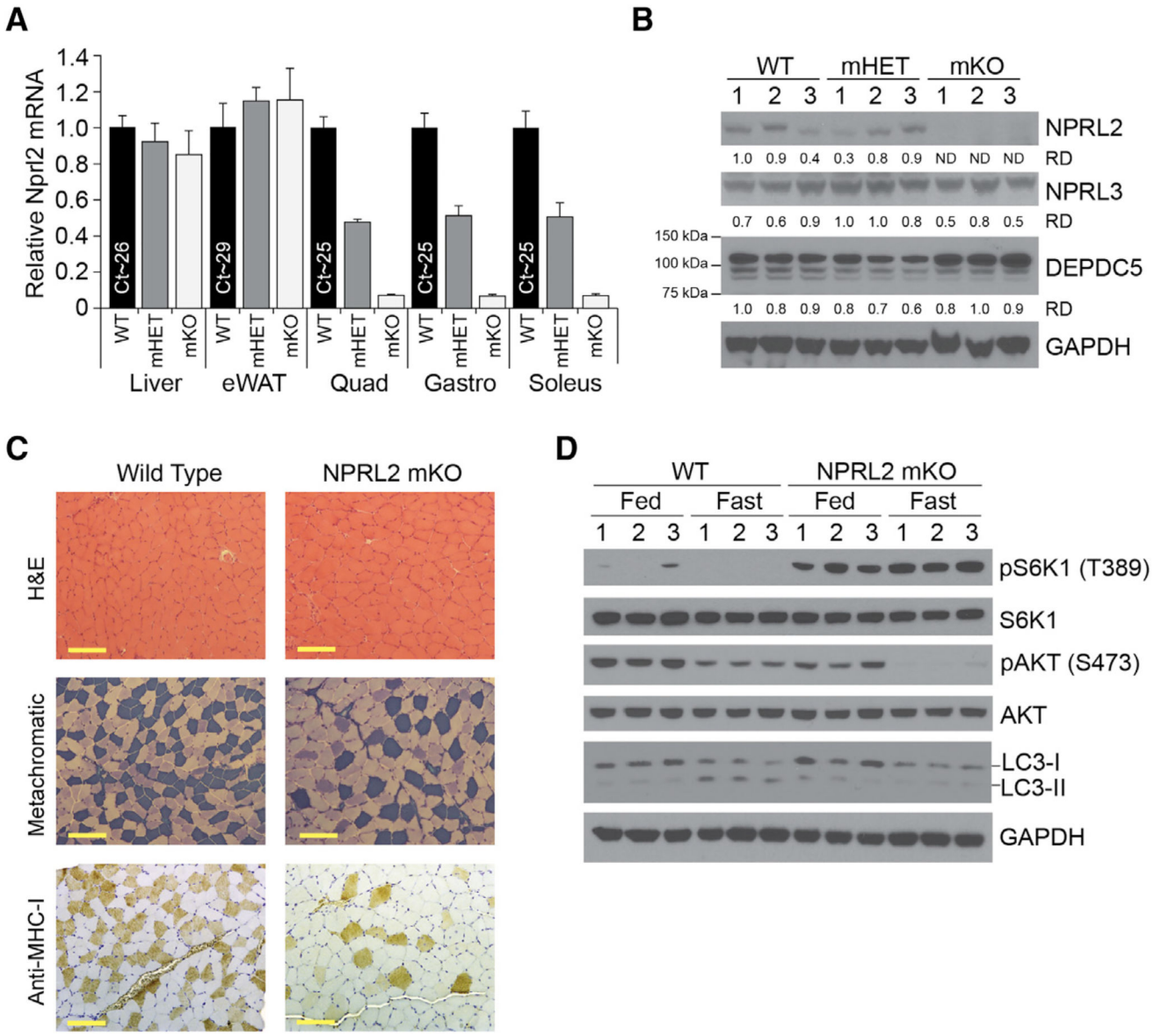

Figure 1. Loss of NPRL2 Alters Muscle Fiber Composition and mTORC1 Activity

(A) qRT-PCR analysis of *Nprl2* mRNA in liver, epididymal white adipose tissue (eWAT), quadricep femoris (quad), gastrocnemius (gastro), and soleus of 2-month-old WT and NPRL2 mHET and NPRL2 mKO male mice. Expression of U36B4 mRNA was used as an internal control. Error bars represent the mean ± SEM (n = 10/3/5 per genotype). Cycle threshold (Ct) values are indicated for comparative expression across tissues.

(B) Western blot analysis of NPRL2, NPRL3, and DEPDC5 in WT, NPRL2 mHET, and NPRL2 mKO in the soleus of 2-month-old male mice. GAPDH was used as loading control (n = 3 mice per genotype). RD, relative density of target protein to GAPDH density; ND, not detected.

(C) Representative H&E, metachromatic dye-ATPase, and slow muscle myosin (MHC class I) immunohistochemistry of WT and NPRL2 mKO soleus tissue sections. Scale bar, 50 μm.

(D) Western blot analysis of pS6K1 (T389), S6K1, pAKT (S473), AKT, LC3-I/LC3-II, and GAPDH from control and NPRL2 mKO mice harvested in the fed and fasted states (24-hr food restriction; n = 3 per group).

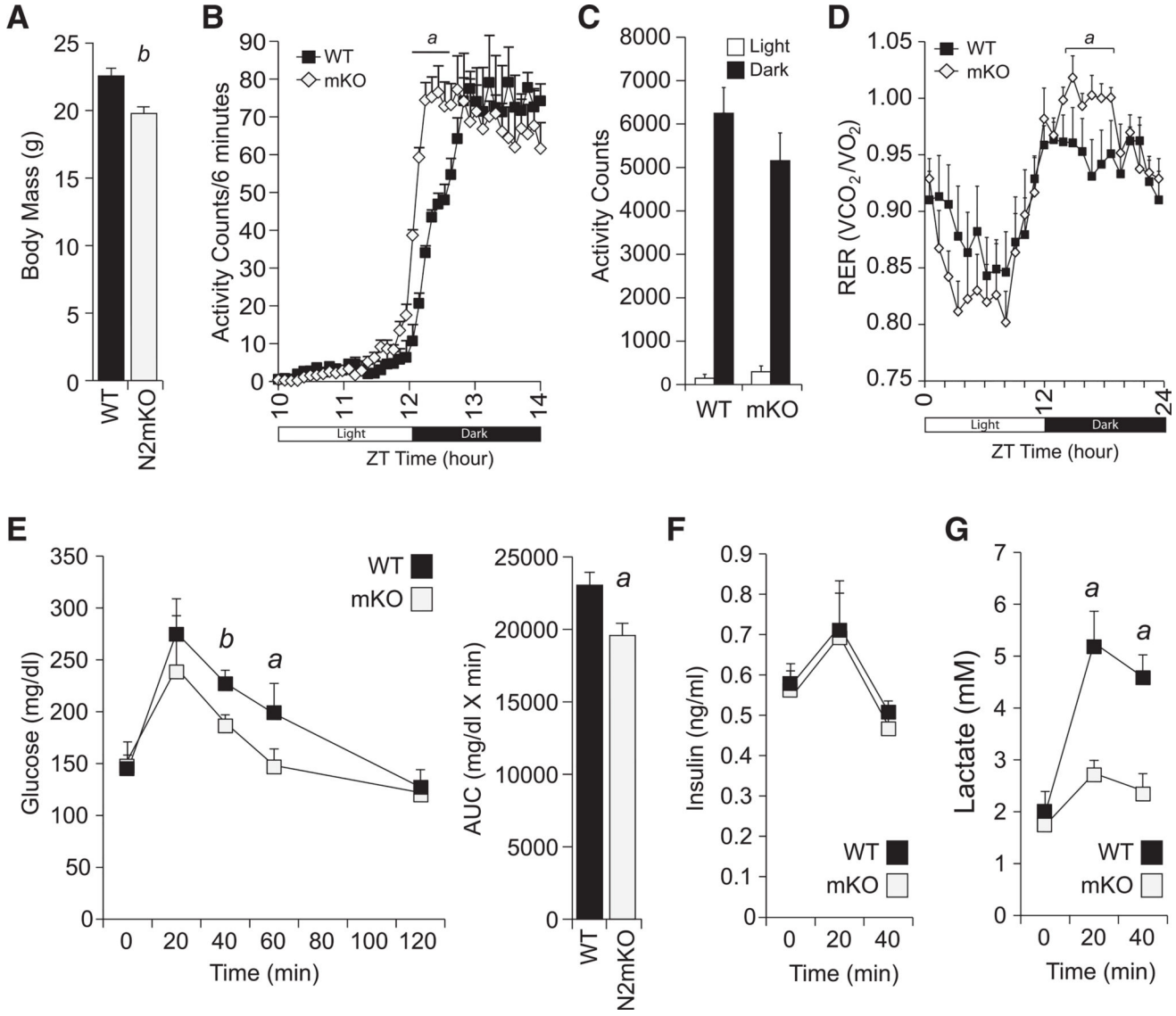

Figure 2. Altered Running Behavior and Carbohydrate Metabolism in NPRL2 mKO

(A) Body mass of 2-month-old WT and NPRL2 mKO males (n = 10/5 mice per genotype, respectively).

(B) Average wheel-running activity over a 2-week period of 2- to 3-month-old male WT and NPRL2 mKO mice taken 2 hr before and after switching from light to dark. Activity counts were taken at 6-min intervals. Error bars represent the mean ± SEM. WT versus NPRL2 mKO (n = 7/4 mice per genotype).

(C) Average daily wheel-running activity measured over 2 weeks during the 12 hr light-to-dark cycle. Error bars represent the mean ± SEM (n = 7/4 mice per genotype).

(D) Metabolic cage analysis of respiratory exchange ratio (RER) of 3-month-old male mice averaged over a 2-day period. Note increased carbohydrate utilization in the dark phase in NPRL2 mKO mice (n = 4 mice per genotype).

(E) Plasma glucose concentration for glucose tolerance test in mice fasted for 4 hr (n = 5 mice per genotype).

(F) Plasma insulin concentrations during the glucose tolerance test.

(G) Plasma lactate levels during the glucose tolerance test.

a, $p < 0.05$; *b*, $p < 0.01$.

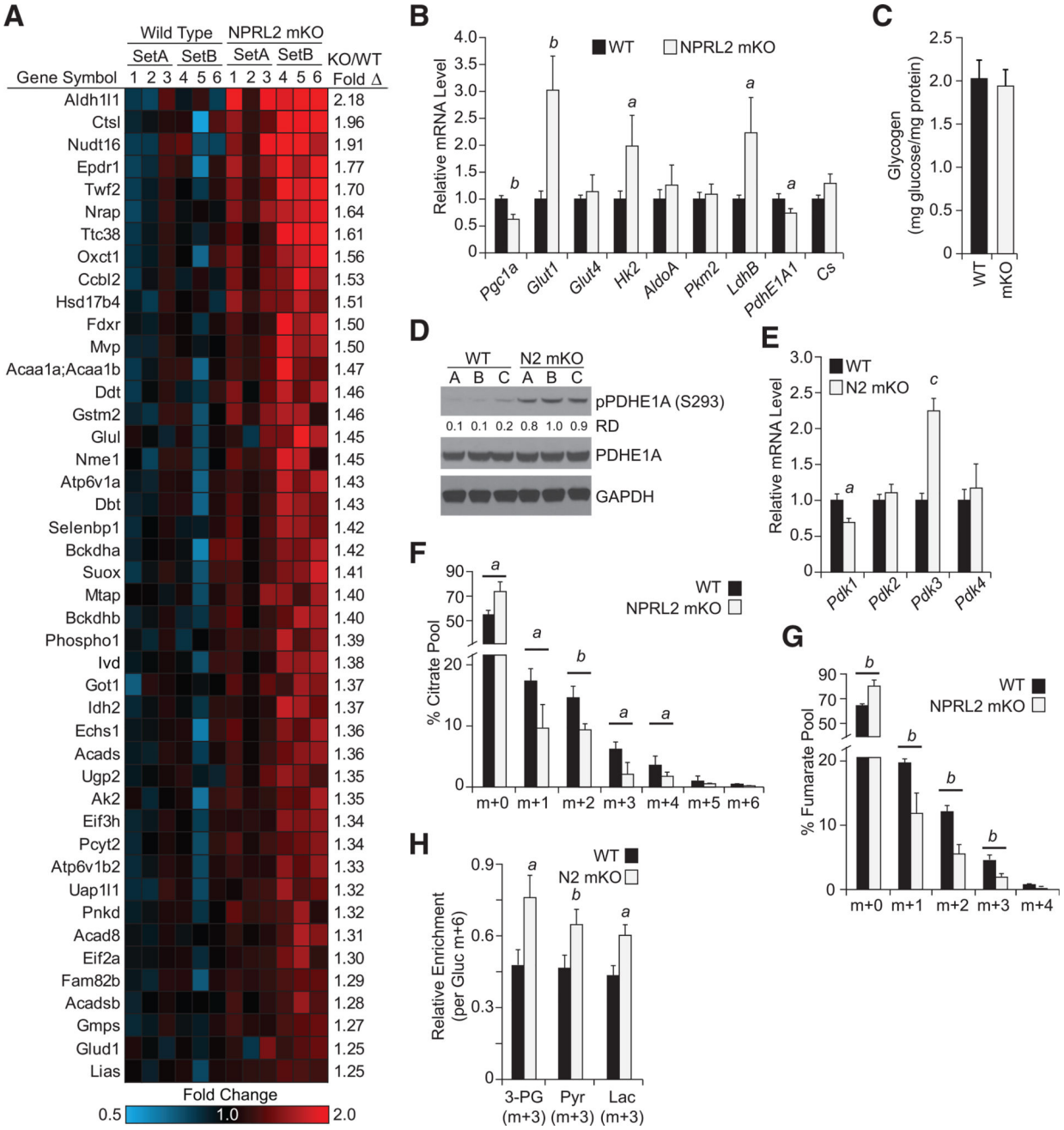

Figure 3. NPRL2 mKO Mice Show Hallmarks of Aerobic Glycolysis

(A) Protein expression heatmap and fold change from mass spectrometry analysis of WT and NPRL2 mKO soleus muscle. $p < 0.05$ (n = 3 mice per genotype per experimental set). (B) qRT-PCR analysis of PPAR gamma coactivator 1 (*Pgc1*a), glucose transporter 1 (*Glut1*), hexokinase 2 (*Hk2*), aldolase A (*AldoA*), pyruvate kinase M2 (*Pkm2*), lactate dehydrogenase B (*LdhB*), pyruvate dehydrogenase component E1A1 (*Pdhe1a1*), and citrate synthase (*Cs*) in soleus of 2-month-old WT and NPRL2 mKO mice (n = 10/5, respectively). (C) Glycogen content in 3-month-old WT and NPRL2 mKO soleus (n = 4 mice per genotype).

(D) Western blot analysis of phosphorylated (S293) and total pyruvate dehydrogenase complex E1A and of GAPDH in the soleus (n = 3 mice per genotype; RD, relative density of P-PDHE1A to PDHE1A).
(E) qRT-PCR analysis of pyruvate dehydrogenase kinase isoforms 1–4 (*Pdk1–Pdk4*) in the soleus (n = 10/5 mice per genotype).
(F and G) Quantification of ^{13}C-glucose conversion into TCA intermediates (F) citrate and (G) fumarate in the soleus muscle, 1 hr after 2 mg/kg intraperitoneal (i.p.) injection. Measurements of citrate and fumarate were made using GC-MS (n = 4 mice per genotype).
(H) Fractional ^{13}C enrichments of glycolytic metabolites are normalized to enrichment of glucose in the soleus tissue. Enrichment of glycolytic metabolites relative to citrate m+2 and enrichments in liver and serum are shown in Figures S3E–S3G. Average values and SEM are displayed (n = 4 mice per genotype).
a, $p < 0.05$; *b*, $p < 0.01$; *c*, $p < 0.001$.

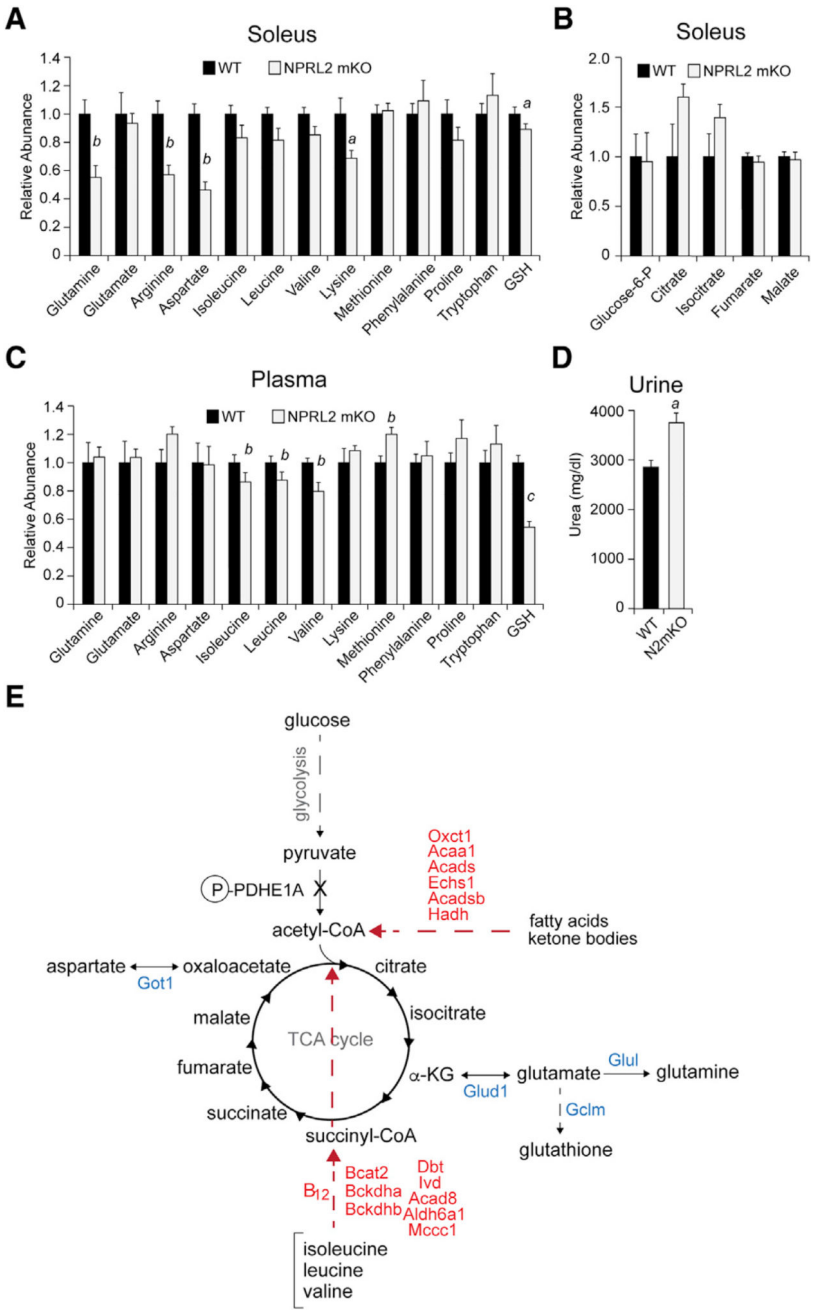

Figure 4. Loss of NPRL2 Alters Amino Acid Metabolism

(A) Relative amino acid abundance in WT and NPRL2 mKO soleus determined by mass spectrometry (n = 4 mice per genotype).

(B) Relative amino acid abundance in WT and NPRL2 mKO plasma determined by mass spectrometry (n = 9/6 mice per genotype, respectively).

(C) Relative TCA cycle intermediate abundance in WT and NPRL2 mKO mice (n = 4 mice per genotype).

(D) Urea content measured in urinary excretion from WT and NPRL2 mKO animals (n = 7/8 per genotype, respectively).

(E) TMT-based quantitation of proteins in soleus in NPRL2 mKO versus WT. Metabolic enzymes that were significantly increased in abundance are shown (blue, cataplerotic reactions; red, anaplerotic reactions). Chronic activation of mTORC1 due to loss of NPRL2 results in a compensatory increase in the indicated amino acid and fatty acid catabolic pathways, many of which feed carbons into the TCA cycle. These findings suggest that NPRL2 and GATOR1 normally function to limit utilization of the mitochondria for biosynthesis and instead promote anaplerotic reactions that restore TCA cycle intermediates for purposes of ATP synthesis.

a, $p < 0.05$; *b*, $p < 0.01$; *c*, $p < 0.001$.